


# An Efficient Maximum Power Point Tracking Controller for Photovoltaic Systems Using Takagi–Sugeno Fuzzy Models

D. Ounnas<sup>1</sup>  · M. Ramdani<sup>2</sup> · S. Chenikher<sup>3</sup> · T. Bouktir<sup>1</sup>

Received: 18 September 2016 / Accepted: 10 April 2017 / Published online: 20 April 2017  
© King Fahd University of Petroleum & Minerals 2017

**Abstract** This paper proposes a new Takagi–Sugeno (T–S) fuzzy model-based maximum power tracking controller to draw the maximum power from a solar photovoltaic (PV) system. A DC–DC boost converter is used to control the output power from the PV panel. Based on the T–S fuzzy model, the fuzzy maximum power point tracking controller is designed by constructing fuzzy gain state feedback controller and an optimal reference model for the optimal PV output voltage, which corresponds actually to maximum power point (MPP). A comparative study with the two base-line controllers of perturb and observe, and the incremental conductance shows that the proposed controller offers fast dynamic response, much less oscillation around MPP, and superior performance.

**Keywords** Photovoltaic (PV) system · Maximum power point tracking (MPPT) · T–S fuzzy model · Linear matrix inequalities (LMIs)

## 1 Introduction

Motivated by environmental concerns and the depletion of fossil fuels, an increased attention has been paid to sustainable energy sources. Fuel cells [1], biomass plants [2],

turbines generators [3,4], and photovoltaic arrays [5,6] represent the most practical and interesting renewable energy systems.

Photovoltaic systems have the advantage of directly converting sunlight into electrical energy by the photovoltaic effect. The generated power can be stored in a battery, used directly or can be connected to a centralized grid [7,8]. As shown in Fig. 1 solar panels have nonlinear power–voltage (P–V) characteristics. The output power depends on temperature, solar radiation and output voltage. Thus, many algorithms and controllers have been proposed in the literature to maximize PV power transfer to various loads. The most important conventional algorithms are perturb and observe (P&O) [9,10], incremental conductance (InCond) [10–12] and hill climbing (HC) [13,14]. These algorithms are widely used in commercial PV panels due to their simplicity, low cost and easy implementation, but on the other hand they suffer from serious drawbacks such as slow tracking of MPP during a rapid change of atmospheric conditions and considerable oscillation around the MPP [15]. A comparative study of P&O, InCond and HC carried out in [16] concluded that these methods are actually equivalent and deliver similar performance.

In order to overcome these drawbacks, many algorithms and control strategies have been proposed: open-circuit voltage (OCV), short-circuit current (SCC) [17] and artificial intelligence (AI)-based methods [18]. The OCV and SCC algorithms are unable to find the true MPP due to the approximation used in these algorithms. In [19], a modified P&O algorithm has been investigated to improve the conventional one. This algorithm is made up by adding the change in the PV current as a third test in its flowchart. In [20], particle swarm optimization (PSO) has been employed as an AI technique to reduce the oscillation in the different steady states of the PV system. In [21–23], the conventional P&O algo-

✉ D. Ounnas  
djamel.ounnas@univ-tebessa.dz

<sup>1</sup> Department of Electrotechnic, Faculty of Technology, University of Setif 1, 19000 Maabouda, Setif, Algeria

<sup>2</sup> LASA Laboratory, Department of Electronics, Faculty of Engineering, University Badji-Mokhtar of Annaba, P.O. Box 12, 23000 Annaba, Algeria

<sup>3</sup> LABGET Laboratory, Department of Electrical Engineering, Faculty of Science and Technology, University of Tebessa, Route de Constantine, 12002 Tebessa, Algeria

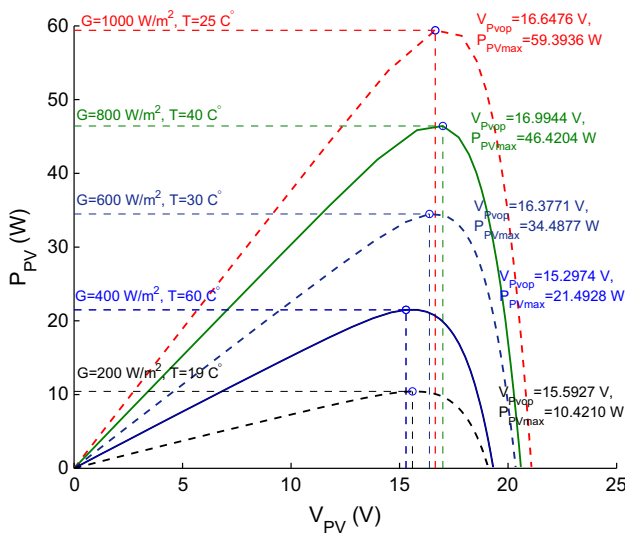


Fig. 1 Power–voltage characteristic of a PV panel

rithm has been combined with Mamdani-type fuzzy logic control (FLC) to develop MPPT-based controllers that have fast time response, less overshoot and more stable operation, whereas, in [24], the output power and voltage variations have been utilized as inputs for a FLC-based MPPT controller to generate the appropriate signal control. In [25], A hybrid fuzzy-neural MPPT controller has been proposed to reduce the oscillation around MPP, where the neural network training data are optimized by genetic algorithm. In [26–29], adaptive neuro-fuzzy inference system (ANFIS)-based MPPT controllers have been proposed to estimate the MPP using a database constructed from a number of experiments performed in various environmental conditions. These controllers use short-circuit current and open-circuit voltage, or cell temperature and solar irradiation, to find MPP using fuzzy inference system (FIS) that is tuned by adaptive neural network (ANN).

On the other hand, many fuzzy MPPT controllers have been proposed based on Takagi–Sugeno (T–S) fuzzy models in the last years [30–34]. The main idea behind the T–S fuzzy models is to describe the processes by an aggregation of linear models. This allows the construction of the fuzzy controller using parallel distributed compensation (PDC) technique [35]. The fuzzy controller gains are calculated based on the stability conditions of the augmented T–S fuzzy system, which can be easily transformed into linear matrix inequalities (LMIs) and solved efficiently by convex programming techniques [36]. In [30], the conventional InCond algorithm has been employed to find the reference voltage and then, combined with a T–S MPPT-based-fuzzy controller, while in [31,32], the reference voltage has been calculated using a T–S reference model uses the measurement of temperature and irradiation as inputs. In [34], a MPP searching algorithm has been proposed based on the evaluation of different lev-

els of irradiation and temperature. The algorithm computes instantly the partial derivative of power with respect to PV cell current and then generate the desired reference state to be tracked using a PDC controller.

In this paper, a new MPPT controller based on T–S fuzzy models is proposed to effectively eliminate the oscillation in the different steady states of the PV system, and thereby ensuring less overshoot and fast time response. The proposed fuzzy control strategy is summarized as follows: First, the nonlinear model of PV system is used to design the T–S fuzzy controller. Next, an optimal reference model is derived according to the optimal PV voltage which is generated using an ANFIS algorithm uses the cell temperature and solar irradiation, as inputs. Finally, a nonlinear tracking controller is developed using the designed T–S fuzzy controller and the optimal reference model. The stability of the augmented system is analyzed by Lyapunov’s method and described by LMI expressions.

The remainder of this paper is organized as follows; in the second section, details about PV conversion system modeling and the influence of climatic parameters on the PV power–voltage characteristic are introduced. In the third section, the proposed MPPT control strategy, which includes three main blocks, is introduced. The first part is dedicated to T–S fuzzy controller and stability analysis conditions, whereas the second part is focused on computing the optimal reference model and nonlinear tracking controller. The simulation results are presented in Sect. 4, followed by a conclusion at the end of the paper.

## 2 PV System Modeling

The considered PV system is composed of DC (Direct Current) load, DC/DC boost converter and PV panel, as shown in Fig. 2. In this study, the following PV system parameters will be used:

- $V_{PV}$  and  $i_{PV}$  are the PV output voltage and current, respectively.

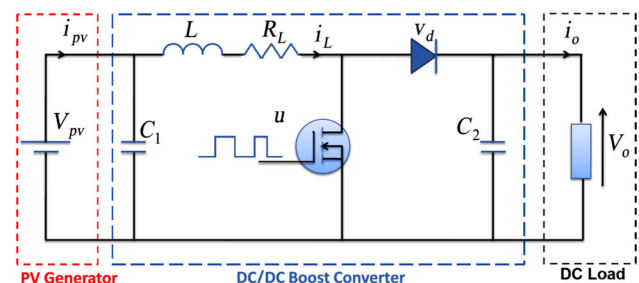


Fig. 2 Photovoltaic system

- $i_L, i_o, V_o$  and  $u$  are the boost self-inductance current, output load current, output load voltage and control input corresponding to the duty cycle, respectively.
- $C_1, C_2, L, R_L, R_m$  and  $v_d$  are the input capacitor, output capacitor, boost inductance, resistance of self-inductance, resistance characterizing the loss through the IGBT and diode’s forward voltage, respectively.

### 2.1 PV Panel Model

The PV output current is given by [37,38]:

$$i_{PV} = n_p I_{ph} - n_p I_s \left( \exp \left[ \frac{q(V_{PV} + R_s i_{PV})}{kTA} \right] - 1 \right) - \frac{V_{PV} + i_{PV} R_s}{R_{sh}} \tag{1}$$

where  $I_{ph}$  and  $I_s$  represent the light-generated current and cell saturation of dark current, respectively.  $R_s$  and  $R_{sh}$  are the cell series and shunt resistances, respectively.  $q, k, T, n_p$  and  $A$  are the electron charge, Boltzmann constant, cell temperature, number of parallel solar cells and the ideal factor, respectively (Fig. 3).

The light-generated current depends on solar irradiation and cell temperature with the following expression:

$$I_{ph} = G (I_{sc} + K_I(T - T_r)) \tag{2}$$

where  $I_{sc}$  represents the cell short-circuit current at 25 °C and 1 kW/m<sup>2</sup>.  $K_I, T_r$  and  $G$  are the cell short-circuit current temperature coefficient, cell reference temperature and solar irradiation in kW/m<sup>2</sup>, respectively. On the other hand, the saturation current depends on cell temperature according to the following expression:

$$I_s = I_{rs} \left( \frac{T}{T_r} \right)^3 \exp \left[ \frac{qE_g}{kA} \left( \frac{1}{T_r} - \frac{1}{T} \right) \right] \tag{3}$$

where  $E_g$  is the band-gap energy of the semiconductor used in the cell and  $I_{rs}$  is the reverse saturation current given by:

$$I_{rs} = \frac{I_{sc}}{\exp \left[ \frac{qV_{oc}}{n_s kAT} \right] - 1} \tag{4}$$

where  $V_{oc}$  is the open-circuit voltage.

The power–voltage characteristic illustrated in Fig. 1 shows that the variation of the maximum power of PV panel ( $P_{PVmax}$ ), which corresponds to an optimal PV output voltage ( $V_{PVop}$ ), highly changes as a function of the solar irradiation and cell temperature.

### 2.2 Boost Converter Model

According to Fig. 2, the dynamic model of the DC/DC boost converter is described by the following equations:

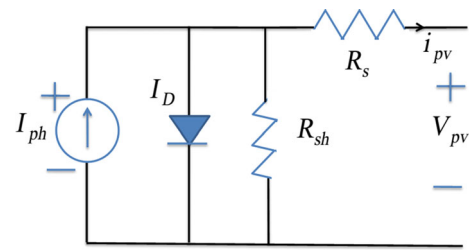


Fig. 3 Electrical equivalent schema of PV panel

$$\begin{cases} \dot{i}_L = -\frac{R_L}{L} i_L + \frac{1}{L} V_{PV} - \frac{1-u}{L} (V_o + v_d - R_m i_L) \\ \dot{V}_{PV} = -\frac{1}{C_1} i_L + \frac{1}{C_1} i_{PV} \end{cases} \tag{5}$$

It should be noted here that the diode’s forward voltage  $v_d$  and the internal resistance  $R_m$  have not been considered in many previous MPPT works, which can affect the regulation of the PV system. In other words, this work considers a more general case.

Using Eqs. (5) and including a new state variable, such as  $\dot{u} = u_{PV}$ , the PV system can be described by the following nonlinear model:

$$\dot{x}(t) = f(x(t)) + Bu(t) + \eta(t) \tag{6}$$

where

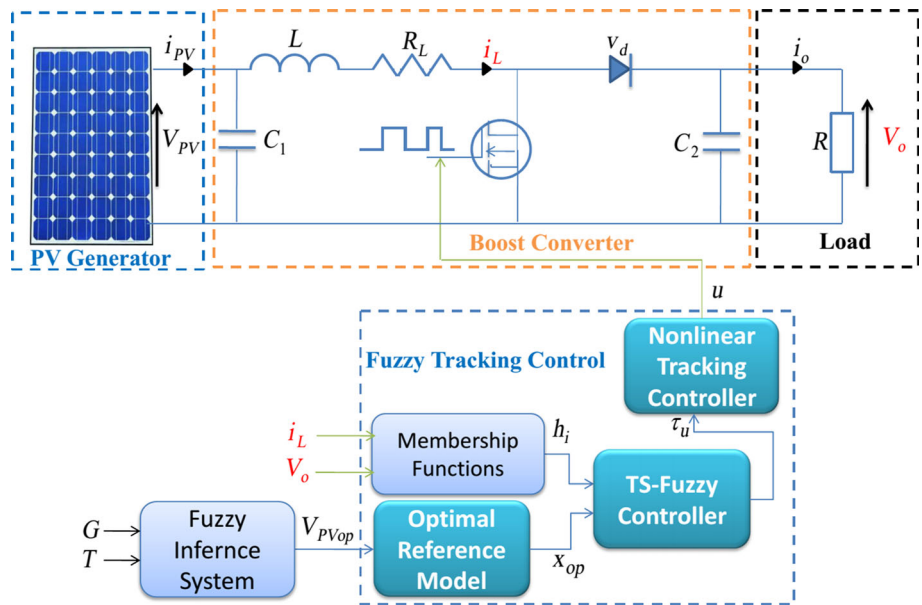
$$f(x(t)) = \begin{bmatrix} -\frac{R_L}{L} i_L + \frac{1}{L} V_{PV} + \frac{V_o + v_d - R_m i_L}{L} u_{PV} \\ -\frac{1}{C_1} i_L \\ 0 \end{bmatrix},$$

$$x = \begin{bmatrix} i_L \\ V_{PV} \\ u_{PV} \end{bmatrix}, \quad B = \begin{bmatrix} 0 \\ 0 \\ 1 \end{bmatrix}, \quad \eta = \begin{bmatrix} -\frac{V_o + v_d}{L} \\ \frac{1}{C_1} i_{PV} \\ 0 \end{bmatrix}.$$

### 3 Proposed Fuzzy Control Method

The objective of this work is to design a fuzzy controller that allows to maximize the power derived from the PV panel. Then, the role of the controller is to ensure that the PV system states  $x = [i_L \ V_{PV} \ u_{PV}]^T$  tracks an optimal trajectory  $x_{op} = [i_{Lop} \ V_{PVop} \ u_{PVop}]^T$  under variable weather conditions. The first step is to develop the fuzzy controller (FC) based on the T–S fuzzy model of the PV system. Next, a nonlinear tracking controller (NTC) and optimal reference model (ORM) are designed according to an optimal voltage calculated using a fuzzy inference system. Thus, a new control scheme with FC, NTC and ORM is proposed, as illustrated in Fig. 4.

**Fig. 4** Proposed MPPT-based T–S fuzzy control scheme



**3.1 T–S Fuzzy system of the PV System**

In order to develop the fuzzy controller, the PV nonlinear model (6) is transformed into T–S fuzzy model using the output load voltage  $V_o$  and the boost inductance current  $i_L$  as decision variables. This leads to the following nonlinear state space form:

$$\dot{x}(t) = A(i_L, V_o)x(t) + Bu(t) + \eta(t) \tag{7}$$

where

$$A(i_L, V_o) = \begin{bmatrix} -\frac{R}{L} & \frac{1}{L} & \frac{V_o + v_d - R_m i_L}{L} \\ -\frac{1}{C_1} & 0 & 0 \\ 0 & 0 & 0 \end{bmatrix}, \quad B = \begin{bmatrix} 0 \\ 0 \\ 1 \end{bmatrix},$$

$$\eta = \begin{bmatrix} -\frac{V_o + v_d}{L} \\ \frac{1}{C_1} i_{PV} \\ 0 \end{bmatrix}.$$

Assuming that the measurable variables  $i_L$  and  $V_o$  are bounded as:

$$\underline{i}_L \leq i_L \leq \bar{i}_L, \quad \underline{V}_o \leq V_o \leq \bar{V}_o \tag{8}$$

and using sector nonlinearity transformation [39], the nonlinear system (7) can be described by a T–S model with  $r = 2^n = 2^2$  fuzzy if–then rules, as follows:

Rule  $i$  : If  $z_1(t)$  is  $F_{1i}$  and  $z_2(t)$  is  $F_{2i}$  Then

$$\dot{x}(t) = A_i x(t) + B_i u(t) + \eta(t), \quad i = 1, \dots, 4$$

where  $z_1 = i_L$  and  $z_2 = V_o$  are the premise variables,  $F_{11}$ ,  $F_{12}$ ,  $F_{21}$  and  $F_{22}$  are the membership functions given by:

$$\begin{cases} F_{11}(i_L) = \frac{i_L(t) - \underline{i}_L}{\bar{i}_L - \underline{i}_L}, & F_{12}(i_L) = 1 - F_{11}(i_L) \\ F_{21}(V_o) = \frac{V_o(t) - \underline{V}_o}{\bar{V}_o - \underline{V}_o}, & F_{22}(V_o) = 1 - F_{21}(V_o) \end{cases} \tag{9}$$

The matrices of the local models are defined as:

$$A_1 = \begin{bmatrix} -\frac{R}{L} & \frac{1}{L} & \frac{\bar{V}_o + v_d - R_m \bar{i}_L}{L} \\ -\frac{1}{C_1} & 0 & 0 \\ 0 & 0 & 0 \end{bmatrix},$$

$$A_2 = \begin{bmatrix} -\frac{R}{L} & \frac{1}{L} & \frac{V_o + v_d - R_m \bar{i}_L}{L} \\ -\frac{1}{C_1} & 0 & 0 \\ 0 & 0 & 0 \end{bmatrix},$$

$$A_3 = \begin{bmatrix} -\frac{R}{L} & \frac{1}{L} & \frac{\bar{V}_o + v_d - R_m \underline{i}_L}{L} \\ -\frac{1}{C_1} & 0 & 0 \\ 0 & 0 & 0 \end{bmatrix},$$

$$A_4 = \begin{bmatrix} -\frac{R}{L} & \frac{1}{L} & \frac{V_o + v_d - R_m \underline{i}_L}{L} \\ -\frac{1}{C_1} & 0 & 0 \\ 0 & 0 & 0 \end{bmatrix},$$

$$B_1 = B_2 = B_3 = B_4 = \begin{bmatrix} 0 \\ 0 \\ 1 \end{bmatrix}.$$

Using the product-inference rule, singleton fuzzifier, and the center of gravity defuzzifier, the overall output of the fuzzy rule-based system is given by:

$$\dot{x}(t) = \sum_{i=1}^r h_i(z(t)) (A_i x(t) + B_i u(t)) + \eta(t) \tag{10}$$

where  $h_i(z) = \omega_i(z) / \sum_{i=1}^r \omega_i(z)$ ,  $\omega_i(z) = \prod_{j=1}^n F_{ij}(z_j)$  for all  $t > 0$ ,  $h_i(z) \geq 0$  and  $\sum_{i=1}^r h_i(z) = 1$ .

### 3.2 T-S Fuzzy Controller and Stability Analysis

The objective is to design a fuzzy controller capable of driving the state of the PV system  $x(t)$  to track an optimal reference model  $x_{op}(t)$ . Then, the feedback tracking control is required to satisfy:

$$x(t) - x_{op}(t) \rightarrow 0 \text{ as } t \rightarrow \infty \tag{11}$$

Let  $\tilde{x}(t) = x(t) - x_{op}(t)$  be defined as the tracking error and its time derivative is given by:

$$\dot{\tilde{x}}(t) = \dot{x}(t) - \dot{x}_{op}(t) \tag{12}$$

Replacing Eq. (10) by its value in (12) and adding the term  $\sum_{i=1}^r h_i A_i (x_{op} - x_{op})$ , Eq. (12) becomes:

$$\dot{\tilde{x}}(t) = \sum_{i=1}^r h_i (A_i \tilde{x} + B_i u + A_i x_{op}) + \eta(t) - \dot{x}_{op}(t) \tag{13}$$

By introducing a new control variable  $\tau_u(t)$  that satisfies the following relation:

$$\sum_{i=1}^r h_i B_i \tau_u = \sum_{i=1}^r h_i(z) (A_i x_{op} + B_i u) + \eta - \dot{x}_{op} \tag{14}$$

and using Eq. (14), the tracking error system (13) can be rewritten as follows:

$$\dot{\tilde{x}}(t) = \sum_{i=1}^r h_i(z(t))(A_i \tilde{x}(t) + B_i \tau_u(t)) \tag{15}$$

The state feedback controllers are designed to deal with the tracking control problem as:

Controller rule  $i$  : If  $z_1(t)$  is  $F_{1i}$  and  $z_2(t)$  is  $F_{2i}$  Then

$$\tau_u(t) = -K_i \tilde{x}(t)$$

The final output of the fuzzy controller is given by the following summation:

$$\tau_u(t) = - \sum_{i=1}^r h_i(z(t)) K_i \tilde{x}(t) \tag{16}$$

Applying control law (16) to model (15), the closed-loop system takes the following form:

$$\dot{\tilde{x}}(t) = \sum_{i=1}^r \sum_{j=1}^r h_i(z(t)) h_j(z(t)) (A_i - B_i K_j) \tilde{x}(t) \tag{17}$$

By letting  $G_{ij} = (A_i - B_i K_j)$ , Eq. (17) can be written as follows:

$$\dot{\tilde{x}}(t) = \sum_{i=1}^r \sum_{j=1}^r h_i(z(t)) h_j(z(t)) G_{ij} \tilde{x}(t) \tag{18}$$

**Stability Analysis.** In order to calculate the T-S fuzzy controller gains  $K_i$ , the following theorem is considered [40,41]:

**Theorem 1** *The equilibrium of continuous fuzzy control system described by (18) is globally asymptotically stable if there exists a common positive definite matrix  $P > 0$ , a diagonal matrix  $D$  and matrices  $Q_{ij}$  with:  $Q_{ii} = Q_{ii}^T$  and  $Q_{ji} = Q_{ij}^T$  for  $i \neq j$ , such that:*

$$G_{ii}^T P + P G_{ii} + Q_{ii} + D P D < 0, i = 1, \dots, r \tag{19}$$

$$\left( \frac{G_{ij} + G_{ji}}{2} \right)^T P + P \left( \frac{G_{ij} + G_{ji}}{2} \right) + Q_{ij} \leq 0, i < j \leq r \tag{20}$$

$$\begin{bmatrix} Q_{11} & Q_{12} & \dots & Q_{1r} \\ Q_{12} & Q_{22} & \dots & Q_{2r} \\ \vdots & \ddots & \ddots & \vdots \\ Q_{1r} & Q_{2r} & \dots & Q_{rr} \end{bmatrix} \equiv \tilde{Q} > 0 \tag{21}$$

for  $i, j = 1, \dots, r$ , s.t. the pairs  $(i, j)$  such that:  $h_i(z) h_j(z) = 0, \forall t$ .

The conditions of the previous theorem can be transformed into LMIs. This transformation corresponds to simple objective changes of variables  $X = P^{-1}$ ,  $K_i = M_i X^{-1}$  and the use of a congruence in inequalities (19), (20), (21). Then, the following LMIs in variables  $X$  and  $M_i$  are obtained:

$$\exists X = X^T > 0, \exists Y_{ii} = Y_{ii}^T, \exists Y_{ij} = Y_{ji}^T, \exists M_i : \begin{bmatrix} X A_i^T + A_i X - B_i M_i - M_i^T B_i^T + Y_{ii} & X D^T \\ D X & -X \end{bmatrix} < 0, \tag{22}$$

$$X A_i^T + A_i X + X A_j^T + A_j X - B_i M_j - M_j^T B_i^T - B_j M_i - M_i^T B_j^T + 2Y_{ij} \leq 0, i < i \leq r \tag{23}$$

$$\begin{bmatrix} Y_{11} & Y_{12} & \dots & Y_{1r} \\ Y_{12} & Y_{22} & \dots & Y_{2r} \\ \vdots & \ddots & \ddots & \vdots \\ Y_{1r} & Y_{2r} & \dots & Y_{rr} \end{bmatrix} \equiv \tilde{Y} > 0 \tag{24}$$

### 3.3 Nonlinear Controller and Optimal Reference Model

The nonlinear tracking controller law  $u(t)$  and optimal reference model variables  $x_{op}(t)$  can be obtained using Eq. (14) which is rewritten as follows:

$$\sum_{i=1}^r h_i B_i (u - \tau_u) = - \sum_{i=1}^r h_i A_i x_{op} - \eta + \dot{x}_{op} \tag{25}$$

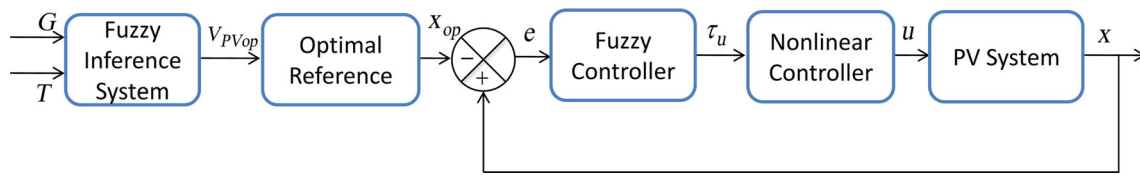


**Fig. 5** Diagram of the control strategy

Noting that:

$$A(i_L, V_o) = \sum_{i=1}^r h_i A_i, \quad B = \sum_{i=1}^r h_i B_i \quad (26)$$

Then, Eq. (25) can be rewritten as the following compact form:

$$B(u - \tau_u) = -A(i_L, V_o)x_{op} - \eta + \dot{x}_{op} \quad (27)$$

In the matrix form, (27) can be written as:

$$\begin{bmatrix} 0 \\ 0 \\ 1 \end{bmatrix} (u - \tau_u) = - \begin{bmatrix} -\frac{R}{L} & \frac{1}{L} & \alpha \\ -\frac{1}{C_1} & 0 & 0 \\ 0 & 0 & 0 \end{bmatrix} \begin{bmatrix} i_{Lop} \\ V_{PVop} \\ u_{PVop} \end{bmatrix} - \begin{bmatrix} -\beta \\ \frac{1}{C_1} i_{PV} \\ 0 \end{bmatrix} + \frac{d}{dt} \begin{bmatrix} i_{Lop} \\ V_{PVop} \\ u_{PVop} \end{bmatrix} \quad (28)$$

where

$$\alpha = \frac{V_o + v_d - R_m i_L}{L}, \quad \beta = \frac{V_o + v_d}{L}$$

It should be noted here that the optimal reference and non-linear controller will be computed according to the optimal voltage reference.

It follows from the second equation of (28) that:

$$i_{Lop}(V_{PVop}) = i_{PV} - C_1 \dot{V}_{PVop} \quad (29)$$

and from the first equation of (28) that:

$$u_{PVop}(V_{PVop}) = \frac{1}{\alpha} \left( \frac{R}{L} i_{Lop} - \frac{1}{L} V_{PVop} + \beta + \dot{i}_{Lop} \right) \quad (30)$$

The nonlinear tracking control can be obtained from the third equation of (28), as follows:

$$u(V_{PVop}) = \dot{u}_{PVop}(V_{PVop}) + \tau_u \quad (31)$$

Figure 5 outlines the layout of the proposed PV array controller and its main components. The first block is reserved to compute the optimal voltage reference  $V_{PVop}$  using a fuzzy inference system which uses the measurement of solar radiation  $G$  and cell temperature  $T$ , as inputs. Then,  $V_{PVop}$  is

**Table 1** PV conversion system parameters

Symbol	Quantity	Value
$k$	Boltzmann's constant	1.38e23 J/K
$A$	Ideal factor of PV cell	1.1 V
$R_{sh}$	Shunt resistance	360.002 $\Omega$
$R_s$	Series resistance	0.18 $\Omega$
$n_s$	Cells connected in series	36
$n_p$	Number of module in parallel	1
$T_0$	Temperature reference	298.15 K
$G_0$	Irradiation reference	1000 W/m <sup>2</sup>
$V_{oc}$	Open-circuit voltage	21.6 V
$I_{scn}$	Nominal short-circuit current	3.8 A
$V_{pvn}$	Nominal PV voltage	21 V
$R$	Load resistance	35 $\Omega$
$C_2$	Output capacitor	4 $\mu$ F
$C_1$	Input capacitor	1 mF
$L$	Inductor	40 mH
$R_L$	Resistance of self-inductance	0.5 $\Omega$
$R_m$	Resistance of IGBT characterizing	0.05 $\Omega$
$v_d$	Diode's forward voltage	1.9 V

used by the optimal reference block to generate  $x_{op}$  using Eqs. (29) and (30). Next, based on the error  $e(t)$  between the actual and optimal states, the fuzzy controller block provides the fuzzy control signal using Eq. (16). This signal is employed by the nonlinear controller block using Eq. (31) to generate the final control signal. More details about the fuzzy inference system block will be discussed in the next section.

### 4 Simulation Results

In order to verify the effectiveness and validity of the proposed method, simulation tests have been carried out on a solar power generation system with the parameters given in Table 1. The T-S fuzzy controller gains are calculated by solving the LMIs (22), (23) and (24), as follows:

$$K_1 = [155.0075 \quad -0.6106 \quad 633.6307]$$

$$K_2 = [92.6114 \quad -0.1194 \quad 570.2396]$$

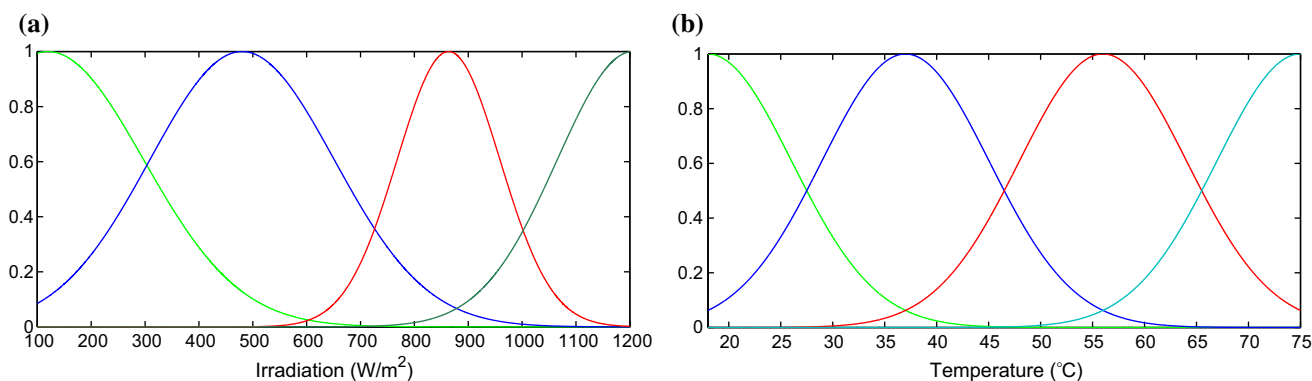


**Fig. 6** Membership functions used by FIS to generate optimal PV voltage. **a** Membership functions of irradiation. **b** Membership functions of temperature

$$K_3 = [282.7187 \quad -0.4403 \quad 616.0382]$$

$$K_4 = [103.4164 \quad 0.3952 \quad 577.9426]$$

where the diagonal matrix is chosen as  $D = [2.75 \ 2.75 \ 2.75]$ .

The optimal voltage corresponding to the maximum power is calculated using MPPT algorithm based on FIS. This MPPT algorithm uses a database constructed from power–voltage characteristic. Part of this database is given in Table 2. By using FIS, the irradiation and temperature are modeled by fuzzy membership functions to get a fuzzy relationship between these parameters and the optimal voltage. These membership functions shown in Fig. 6 are optimized using ANFIS algorithm.

The first test is carried out in various atmospheric conditions where temperature and irradiation are assumed to be as shown in Fig. 7a, b, respectively. The responses of PV output voltage and PV output power provided using the T–S controller are shown in Fig. 7c, d, while the responses of boost converter current and control signal are shown in Fig. 7e, f. As it can be observed, the steady states follow perfectly the optimal trajectories and are not affected by the solar irradiation and cell temperature variations. This leads to an important extraction of the available solar power and an improved performance of the system.

In the second test, the proposed method is compared with the P&O and InCond methods due to their popularity. For the compared methods, fixed perturbation step size of 0.01 s and an update frequency of 22 kHz are chosen using a trade-off between the tracking speed and oscillations in the steady state. The responses of PV output voltage and PV output power are shown in Fig. 8a, b while the responses of PV output current and control signal are shown in Fig. 8c, d. The temperature is assumed to be constant 25 °C while the solar irradiation is assumed to be variable. Table 3 presents the response time and the efficiency tracking ( $E_T$ ) of the three MPPT methods which is defined as [42]:

**Table 2** Part of database used by ANFIS algorithm

Irradiation (W/m <sup>2</sup> )	Temperature (°C)	$V_{PVop}$ (V)
700	30	16.8813
200	45	15.0884
900	35	16.9792
100	50	13.9394
300	60	15.2033
400	25	16.6476
500	23	16.3100
600	20	16.4832
500	23	16.3100

$$E_T = \frac{\int P_{PV} dt}{\int P_{PVmax} dt} \tag{32}$$

where  $P_{PVmax}$  is the theoretical maximum power.

It can be seen that the proposed method has high tracking speed and also has more efficiency than conventional P&O and InCond methods at different levels of irradiation, most notably when the irradiation increases or decreases. Moreover, portions of the steady states in the range of 1–2s is enlarged as illustrated in Fig. 8, to show the efficiency of the proposed controller. It can be clearly seen from the enlarged portions that the responses of steady states with the proposed controller track perfectly their optimum operating points with much less oscillation, whereas the responses of PV system with the compared controllers show a considerable amount of oscillation in the different states. This improves the efficiency and greatly reduces the PV power loss. Although, it is possible to reduce those oscillations by reducing the perturbation step size, but this will result in slower tracking response.

In addition, the performance of the three methods is evaluated using root-mean-square error (RMSE) between the PV

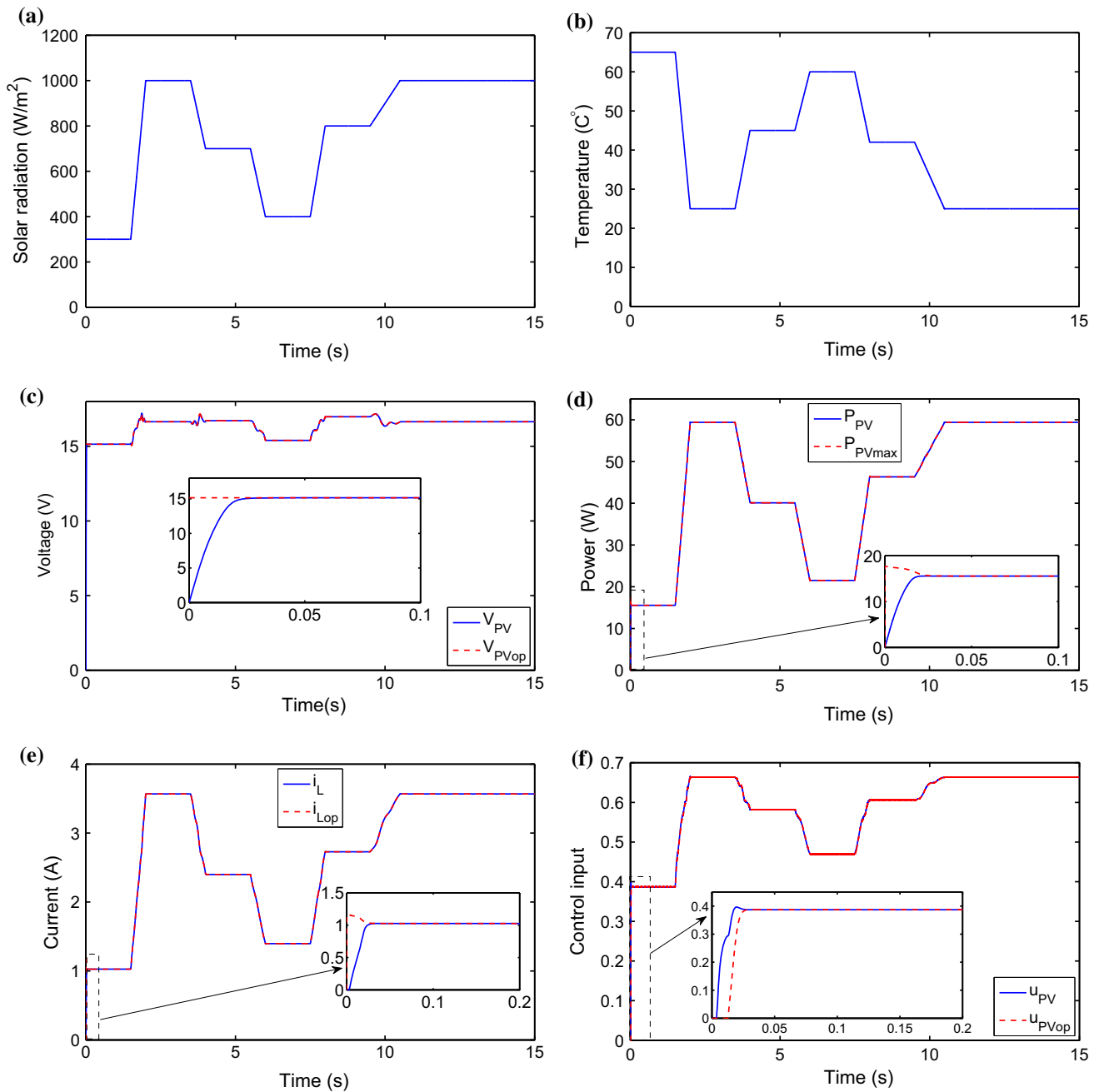


**Fig. 7** Simulation results for various atmospheric conditions. **a** Irradiation profile used to test the proposed method. **b** Temperature profile used to test the proposed method. **c** PV output voltage. **d** PV output power. **e** Inductance current of boost converter. **f** Duty ratio

output power and its theoretical maximum power. The RMSE is defined as follows [43,44]:

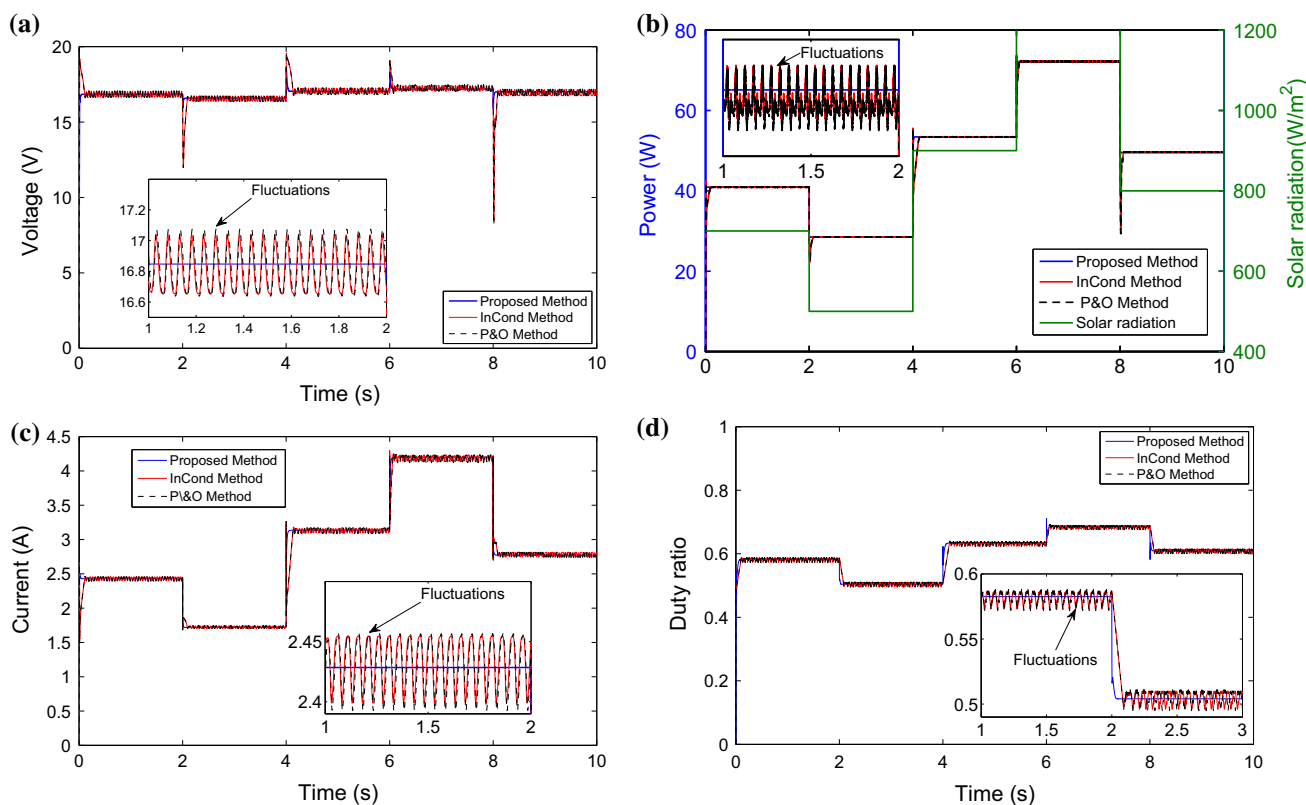
$$RMSE = \sqrt{\frac{\sum_{i=1}^N (P_{PV,i} - P_{PVmax,i})^2}{N}} \quad (33)$$

Figure 9a presents the RMSEs of PV output power at different irradiation levels with a constant temperature of 25 °C, while Fig. 9b shows the RMSEs of PV output power at differ-

ent temperatures with a constant irradiation of 1000 W/m<sup>2</sup>. It is clear that the RMSEs of the compared methods are greater than the preferred one for a wide range of operating conditions. This shows that the proposed controller is able to extract a maximum possible power with much less power loss.

In order to demonstrate the good convergence to the MPPs of the power–voltage characteristics using the proposed method in comparison with P&O and InCond methods,





**Fig. 8** Comparison between P&O, InCond and the proposed fuzzy controllers. **a** PV output voltage. **b** PV output power. **c** PV output current. **d** Duty ratio

**Table 3** Comparison of different MPPT methods

MPPT method	Response time (s)	Efficiency (%)
P&O	0.0791	97.98
InCond	0.0821	97.96
Proposed	0.0078	99.44

simulation tests of power–voltage characteristics of the PV system are carried out in a constant temperature of 25 °C and varying solar radiation:  $500 + 500 \sin(\pi t)$  (W/m<sup>2</sup>). First, the solar radiation is assumed to be increased from 500 to 1000 W/m<sup>2</sup> and then assumed to be decreased from 1000 to 0 W/m<sup>2</sup>. The simulation results are shown in Figs. 10, from which, the following facts could be observed:

- The proposed method guarantees rapid convergence to MPPs when the solar radiation increases from 500 to 1000 W/m<sup>2</sup>, or decreases from 1000 to 0 W/m<sup>2</sup>;
- The compared methods cannot guarantee convergence to MPPs when The solar radiation increases from 500 to 1000 W/m<sup>2</sup>;

- Only the InCond method guarantees convergence to MPPs when the solar radiation decreases from 1000 to 400 W/m<sup>2</sup>;
- The compared methods cannot guaranteed convergence to MPPs when the solar radiation decreases from 400 to 0 W/m<sup>2</sup>.

From the analysis of the power–voltage characteristics in Fig. 10, it can be confirmed that the proposed controller offers fast dynamic response and superior performance in terms of the convergence to the MPPs.

### 5 Conclusion

An efficient T–S fuzzy controller is proposed for maximum power point tracking of photovoltaic conversion system. The proposed controller is able to drive the PV system to track an optimal reference model with fast tracking and much less oscillation in steady states, during rapid changes of weather conditions. The optimal reference model is designed according to the optimal voltage of PV panel which is generated by ANFIS algorithm. The fuzzy controller gains are cal-

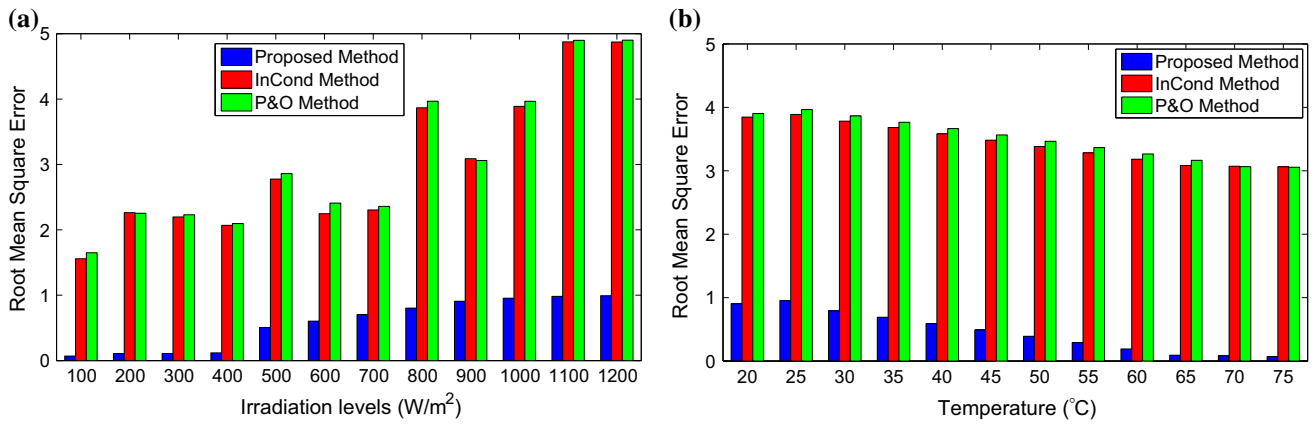


**Fig. 9** Root-mean-square error in PV output power. **a** Error at different irradiances and constant temperature. **b** Error at different temperatures and constant irradiation

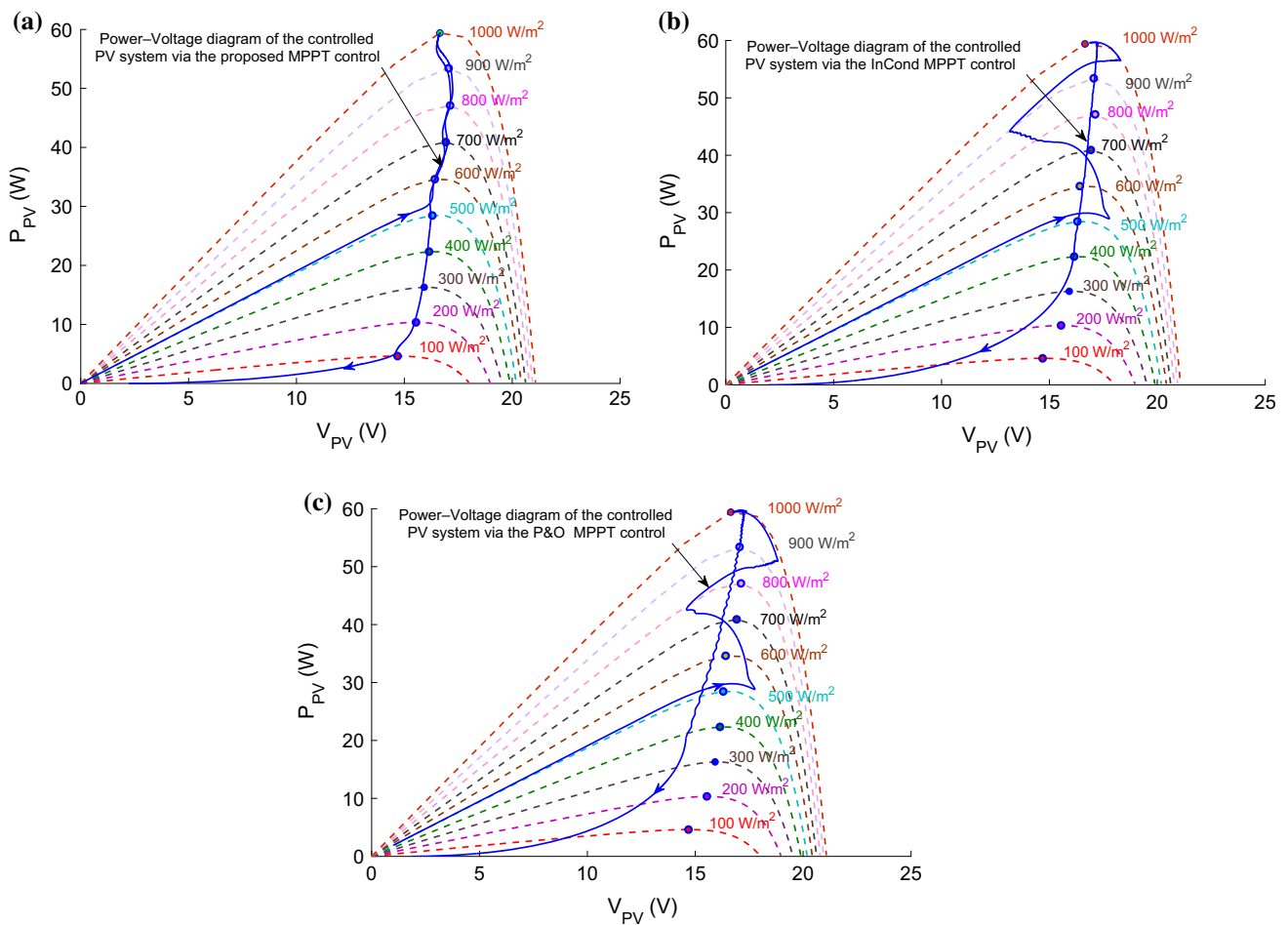


**Fig. 10** P–V characteristic of the PV system via: **a** proposed method; **b** InCond method; **c** P&O method

culated based on sufficient conditions which are given in LMIs form and solved using optimization tools. Simulations results and comparison with conventional P&O and InCond

algorithms show that the PV system can be controlled effectively at different operating regions by the proposed fuzzy tracking control scheme and can overcome the limitations of

conventional controllers. The practical implementation and robustness issue will be the subject of a future research work.

**Acknowledgements** Funding was provided by LABGET Laboratory, Department of Electrical Engineering, Faculty of Technology, University of Tebessa.

## References

- Cossutta, P.; Aguirre, M.P.; Cao, A.; Raffo, S.; Valla, M.I.: Single-stage fuel cell to grid interface with multilevel current-source inverters. *IEEE Trans. Ind. Electron.* **62**(8), 5256–5264 (2015)
- Singh, S.; Subhash, C.K.: Optimal sizing of grid integrated hybrid PV-biomass energy system using artificial bee colony algorithm. *IET Renew. Power Gen.* **10**(5), 642–650 (2016)
- Meghni, B.; Dib, D.; Azar, A.T.; Saadoun, A.: Effective supervisory controller to extend optimal energy management in hybrid wind turbine under energy and reliability constraints. *Int. J. Dynam. Control* 1–15 (2017). doi: [10.1007/s40435-016-0296-0](https://doi.org/10.1007/s40435-016-0296-0)
- Rahim, A.H.M.A.; Khan, M.H.: A swarm-based adaptive neural network SMES control for a permanent magnet wind generator. *Arab. J. Sci. Eng.* **39**(11), 7957–7965 (2014)
- Vincheh, M.R.; Kargar, A.; Markadeh, G.A.: A hybrid control method for maximum power point tracking (MPPT) in Photovoltaic systems. *Arab. J. Sci. Eng.* **39**(6), 4715–4725 (2014)
- Azri, M.; Rahim, N.A.; Elias, M.F.M.: Transformerless DC/AC converter for grid-connected PV power generation system. *Arab. J. Sci. Eng.* **39**(11), 7945–7956 (2014)
- Tipler, P.A.; Mosca, G.: *Physics for Scientist and Engineers*, 6th edn. W.H. Freeman, New York (2008)
- Oladimeji, I.; Nor, Z. Y.; Nordin, S.: Matlab/Simulink model of solar PV array with perturb and observe MPPT for maximising PV array efficiency. In: *Conference on Energy Conversion (CENCON)*. pp. 254–258 (2015)
- Abdelsalam, A.K.; Massoud, A.M.; Ahmed, S.; Enjeti, P.N.: High performance adaptive perturb and observe MPPT technique for photovoltaic-based microgrids. *IEEE Trans. Power Electron.* **26**(4), 1010–1021 (2011)
- Manoj, P.; Amruta, D.: Design and simulation of Perturb and Observe Maximum Power Point Tracking using MATLAB/Simulink. In: *International Conference on Industrial Instrumentation and Control (ICIC)*. pp. 1345–1349 (2015)
- Safari, A.; Mekhilef, S.: Simulation and hardware implementation of incremental conductance MPPT with direct control method using Cuk converter. *IEEE Trans. Ind. Electron.* **58**(4), 1154–1161 (2011)
- Worku, M. Y.; Abido, M. A.: Real-time implementation of grid-connected PV system with decoupled P–Q controllers. In: *Conference on Control and Automation (MED)*. pp. 841–846 (2014)
- Kjaer, S.B.: Evaluation of the hill climbing and the incremental conductance maximum power point trackers for photovoltaic power systems. *IEEE Trans. Energy Convers.* **27**(4), 922–929 (2012)
- Mohammad, I.B.; Pouya, T.; Yousef, M.N.; Ali, K.K.; Paimaneh, S.: Modeling and simulation of hill climbing MPPT algorithm for photovoltaic application. In: *Power Electronics, Electrical Drives, Automation and Motion (SPEEDAM)*, Conference on. pp. 1041–1044 (2016)
- Adel, A.E.; Hamdi, A.; Montaser, A.S.: Implementation of a modified perturb and observe maximum power point tracking algorithm for photovoltaic system using an embedded microcontroller. *IET Renew. Power Gen.* **10**(4), 551–560 (2016)
- Sera, D.; Mathe, L.; Kerekes, T.; Spataru, S.V.; Teodorescu, R.: On the perturb-and-observe and incremental conductance MPPT methods for PV systems. *IEEE J. Photovolt.* **3**(3), 1070–1078 (2013)
- Masoum, M.A.S.; Dehbonei, H.; Fuchs, E.F.: Theoretical and experimental analysis of photovoltaic systems with voltage and current-based maximum power-point tracking. *IEEE Trans. Energy Convers.* **17**(4), 514–522 (2002)
- Mellit, A.; Kalogirou, S.: Artificial intelligence techniques for photovoltaic applications: a review. *Prog. Energy Combust. Sci.* **34**(5), 574632 (2008)
- Belkaid, A.; Colak, I.; Kayisli, K.: Implementation of a modified P&O-MPPT algorithm adapted for varying solar radiation conditions. *Electr. Eng.* pp. 1–8 (2016)
- Ishaque, K.; Salam, Z.; Amjad, M.; Mekhilef, S.: An improved particle swarm optimization (PSO) based MPPT for PV with reduced steady-state oscillation. *IEEE Trans. Power Electron.* **27**(8), 3627–3638 (2012)
- Zainuri, M.A.A.M.; Radzi, M.A.M.; Che Soh, A.; Abd Rahim, N.: Development of adaptive perturb and observe-fuzzy control maximum power point tracking for photovoltaic boost DC–DC converter. *IET Renew. Power Gen.* **8**(2), 183–194 (2014)
- Ahmed, A.; Ali, N.H.; Tshilidzi, M.: Perturb and observe based on fuzzy logic controller maximum power point tracking (MPPT). In: *2014 International Conference on Renewable Energy Research and Application (ICRERA)*. pp. 406–411 (2014)
- Radak, B.; Chitralakha, M.; Anup, K.G.: MPPT of solar photovoltaic cell using perturb & observe and fuzzy logic controller algorithm for buck-boost DC–DC converter. In: *2015 International Conference on Energy, Power and Environment*, pp. 1–5 (2015)
- Liu, C.-L.; Chen, J.-H.; Liu, Y.-H.; Yang, Z.-Z.: An asymmetrical fuzzy-Logic-control-based MPPT algorithm for photovoltaic systems. *Energies* **7**(4), 2178–2193 (2014)
- Vincheh, M.R.; Kargar, A.; Markadeh, G.A.: A hybrid control method for maximum power point tracking (MPPT) in photovoltaic systems. *Arab. J. Sci. Eng.* **39**(6), 4715–4725 (2014)
- Abu-Rub, H.; Iqbal, A.; Moin Ahmed, S.; Peng, F.Z.; Li, Y.; Baoming, G.: Quasi-Z-source inverter-based photovoltaic generation system with maximum power tracking control using ANFIS. *IEEE Trans. Sustain. Energy* **4**(1), 11–20 (2013)
- Afghoul, H.; Krim, F.; Chikouche, D.: Increase the photovoltaic conversion efficiency using neuro-fuzzy control applied to MPPT. In: *Renewable and Sustainable Energy Conference (IRSEC)*. pp. 348–353 (2013)
- Abido, M.A.; Khalid, M.S.; Worku, M.Y.: An efficient ANFIS-based PI controller for maximum power point tracking of PV systems. *Arab. J. Sci. Eng.* **40**(9), 2641–2651 (2015)
- Dragan, M.; Srete, N.: ANFIS as a method for determining MPPT in the photovoltaic system simulated in MATLAB/Simulink. In: *Information and Communication Technology, Electronics and Microelectronics*, pp. 1082–1086 (2015)
- Elkhatib, K.; Abdel, A.: Design of maximum power fuzzy controller for PV systems based on the LMI-based stability. *Intelligent Systems in Technical and Medical Diagnostics*, Volume 230 of the series *Advances in Intelligent Systems and Computing*. pp. 77–88 (2012)
- Abid, H.; Toumi, A.; Chaabane, M.: MPPT algorithm for photovoltaic panel based on augmented TakagiSugeno fuzzy model. *Hindawi Publishing Corporation ISRN Renewable Energy*, Article ID 253146 (2014)
- Abid, H.; Toumi, A.; Chaabane, M.: TS fuzzy algorithm for photovoltaic panel. *Int. J. Fuzzy Syst.* **17**(2), 215–223 (2015)
- Zhang, S.; Wang, T.; Li C., Zhang, J.; Wang, Y.: Maximum power point tracking control of solar power generation systems based on type-2 fuzzy logic. In: *International World Congress on Intelligent Control and Automation*, Guilin, pp. 12–15 (2016)



34. Zayani, H.; Allouche, M.; Kharrat M.; Chaabane M.: Maximum power point tracking control of solar power generation systems based on type-2 fuzzy logic. In: International Conference on Sciences and Techniques of Automatic Control and Computer Engineering, Monastir, Tunisia, December, pp. 21–23 (2016)
35. Tanaka, K.; Wang, H.O.: Fuzzy Control Systems Design and Analysis: A Linear Matrix Inequality Approach. Wiley, New York (2001)
36. Gahinet, P.; Nemirovski, A.; Laub, A.J.; Chilali, M.: LMI Control Toolbox. MathWorks, Natick (1995)
37. Villalva, M.G.; Gazoli, J.R.; Filho, E.R.: Comprehensive approach to modelling and simulation of photovoltaic array. IEEE Trans. Power Electron. **25**(5), 1198–1208 (2009)
38. Ballouti, A.; Djahli, F.; Bendjadou, A.: MPPT system for photovoltaic module connected to battery adapted for unstable atmospheric conditions using VHDL-AMS. Arab. J. Sci. Eng. **36**(3), 2021–2031 (2014)
39. Ohtake, H.; Tanaka, K.; Wang, H.: Fuzzy modeling via sector nonlinearity concept. Integr. Comput. Aided Eng. **10**(4), 333–341 (2003)
40. Lian, K.Y.; Liou, J.: Output tracking control for fuzzy systems via output feedback design. IEEE Trans. Fuzzy Sys. **14**(5), 381–392 (2006)
41. Ounnas, D.; Ramdani, M.; Chenikher, S.; Bouktir, T.: Optimal reference model based fuzzy tracking control for wind energy conversion system. Int. J. Renew. Energy Res. **6**(3), 1129–1136 (2016)
42. Bayod-Rjula, -A.; Cebollero-Abin, J.-A.: A novel MPPT method for PV systems with irradiance measurement. Sol. Energy **109**, 95–104 (2014)
43. Atiqah, H.b M.N.; Ahmad, M.b O.; Hedzlin, b Z.: Modeling and simulation of grid inverter in grid-connected photovoltaic system. Int. J. Renew. Energy Res. **4**(4), 949–957 (2014)
44. Ounnas, D.; Ramdani, M.; Chenikher, S.; Bouktir, T.: A combined methodology of  $H_\infty$  fuzzy tracking control and virtual reference model for a PMSM. Adv. Electr. Electron. Eng. **13**(3), 212–222 (2015)

